Optical Fiber Technology 20 (2014) 513–519

Contents lists available at ScienceDirect

Optical Fiber Technology

www.elsevier.com/locate/yofte

Gain sideband splitting in dispersion oscillating fibers

Christophe Finot [a,*], Fang Feng [a], Yanne Chembo [b], Stefan Wabnitz [c]

[a] Laboratoire Interdisciplinaire Carnot de Bourgogne, UMR 6303 CNRS-Université de Bourgogne, 9 avenue Alain Savary, BP 47870, 21078 Dijon Cedex, France
[b] FEMTO-ST/Optics department, UMR 6174 CNRS-University of Franche-Comté, 16 route de Gray, 25030 Besançon Cedex, France
[c] Dipartimento di Ingegneria dell'Informazione, Università degli Studi di Brescia, via Branze 38, 25123 Brescia, Italy

ARTICLE INFO

Article history:
Received 21 April 2014
Revised 8 June 2014
Available online 10 July 2014

Keywords:
Dispersion oscillating fiber
Modulation instability
Four-wave mixing

ABSTRACT

We analyze the modulation instability spectrum in a varying dispersion optical fiber as a function of the dispersion oscillation amplitude. For large dispersion oscillations, we predict a novel sideband splitting into different sub-sidebands. The emergence of the new sidebands is observed whenever the classical perturbation analysis for parametric resonances predicts vanishing sideband amplitudes. The numerical results are in good quantitative agreement with Floquet or Bloch stability analysis of four-wave mixing in the periodic dispersion fiber. We have also shown that linear gain or loss may have a dramatic influence in reshaping the new sidebands.

© 2014 Elsevier Inc. All rights reserved.

1. Introduction

Modulation instability (MI) is a nonlinear process that has been widely investigated in various fields of physics including plasma, hydrodynamics and optics, to cite a few. In the presence of a high power continuous wave (CW), MI leads to the emergence and amplification of gain sidebands in the wave spectrum. In nonlinear fiber optics, such a process has been demonstrated in fibers with anomalous, constant group velocity dispersion (GVD) [1], as well as in normal GVD fibers by enabling the fulfillment of the nonlinear phase-matching condition through either fourth order dispersion [2], birefringence or a multimodal structure [3,4]. More recently, a renewed experimental and theoretical interest in MI studies has been stimulated by the availability of fibers presenting a longitudinal and periodic modulation of their dispersion properties [5]. Indeed, thanks to the periodic dispersion landscape, which leads to quasi-phase-matching (QPM) of the nonlinear four-wave mixing (FWM) process, MI sidebands can be observed even in the regime of normal average GVD of a dispersion-oscillating optical fiber (DOF) [6–8]. Recent experimental works have confirmed the QPM-induced MI process in the normal GVD regime of microstructured DOF around 1 μm [5], as well as of non-microstructured highly nonlinear DOF at telecom wavelengths [9,10].

To date, the role of the amplitude of the GVD oscillations on the MI spectrum of a DOF remains largely unexplored. In this work, we present a systematic study of the dependence of various sidebands which emerge at the output of a DOF, as the amplitude of the dispersion variations grows progressively larger. We unveil the emergence of new sidebands, as well as their unexpected splitting in sub-sidebands. As we shall see, the emergence of new sidebands may be qualitatively described by extending to a continuum set of frequencies the analytical theory that was established in [11] for a discrete set of sidebands. We also present a detailed study of the influence of optical losses on the profile and splitting of MI sidebands in a DOF.

2. Model and situation under investigation

The evolution of the optical field ψ in an DOF can be described by the nonlinear Schrödinger equation (NLSE) that includes both the Kerr nonlinearity γ and a periodically varying second-order dispersion $\beta_2(z)$

$$i\frac{\partial\psi}{\partial z}-\frac{\beta_2(z)}{2}\frac{\partial^2\psi}{\partial t^2}+\gamma|\psi|^2\psi+i\frac{\alpha}{2}\psi=0 \quad (1)$$

In the last section of this paper, we will also discuss the influence of linear losses that are included through the coefficient α (negative and positive values of α leading to distributed amplification and losses respectively). In Eq. (1) we did not include higher-order dispersion terms or Raman scattering. Nevertheless, we checked that these effects do not have a noticeable influence on the MI spectral dynamics that we are going to describe.

MI induced by the longitudinal variations of chromatic dispersion has been theoretically investigated before in a wide range of configurations, ranging from sinusoidal profiles with a spatial period of a few tens of meters [5,9], up to dispersion-managed systems with periods of several kilometers [6,12–14]. We consider

* Corresponding author.
E-mail address: christophe.finot@u-bourgogne.fr (C. Finot).

http://dx.doi.org/10.1016/j.yofte.2014.06.003
1068-5200/© 2014 Elsevier Inc. All rights reserved.

in this contribution the specific case of DOF whose parameters are inspired by the previous numerical works which were carried out in the context of the transmission of high-speed telecommunication signals in dense dispersion managed links [15]. The fabrication of such a DOF is fully consistent with existing drawing techniques [16]. More precisely, the stepwise dispersion profile over one spatial period Λ of the fiber under study is provided by the map

$$\begin{cases} \beta_2(z) = \beta_{2av} + \beta_{2amps} & \text{if } z < \Lambda/2 \\ \beta_2(z) = \beta_{2av} - \beta_{2amps} & \text{if } z > \Lambda/2 \end{cases} \quad (2)$$

where β_{2av} is the average dispersion of the fiber, and β_{2ampS} is half of the peak-to-peak amplitude of the dispersion variation (the second order dispersion β_2 being related to the dispersion parameter D by $D = -2\pi\ c\ \beta_2/\lambda^2$, λ being the wavelength and c the light velocity). Using a Fourier decomposition, it is possible to decompose the profile (2) into a series of sinus functions having spatial frequencies multiple to $1/\Lambda$. For the sake of simplicity, and since analytical solutions exist for this case, we concentrate here on the fundamental Fourier component, so that we may reduce the stepwise dispersion profile (2) to the following sinusoidal variation

$$\beta_2(z) = \beta_{2av} + \beta_{2amp}\sin(2\pi z/\Lambda) \quad (3)$$

where β_{2amp} is the corresponding amplitude of the dispersion variation: $\beta_{2amp} = 4\ \beta_{2amps}/\pi$.

Let us consider here a DOF with a Kerr nonlinearity of $\gamma = 2\ \mathrm{W}^{-1}\ \mathrm{km}^{-1}$, a spatial period of the dispersion oscillation $\Lambda = 1$ km, and a dispersion average value of $D_{av} = -0.5$ ps/km/nm at the wavelength $\lambda_0 = 1550$ nm. The fiber is pumped by a CW with the average power $P = 0.75$ W at λ_0. The NLSE (1) is numerically solved by the standard split-step Fourier algorithm including a weak input white noise seed, and the results are averaged over 24 shots.

In the presence of sinusoidal longitudinal GVD variations, QPM of FWM or MI leads to the appearance of resonant gain sidebands, whose angular frequency shift relative to the pump can be analytically predicted, by assuming an indefinitely long fiber, as follows [6]:

$$\Omega_p = \pm\sqrt{\frac{2\pi p/\Lambda - 2\gamma P}{\beta_{2av}}} \quad (4)$$

with $p = 1, 2, 3\ldots$. More recently, it has been shown that the gain experienced by the pth sidebands after a propagation length L can be predicted by the formula [11]:

$$G_p^{dB} = 10\ \log_{10}\left\{\exp\left[2\gamma PL\left|J_p\left(\frac{\beta_{2amp}\ \Omega_p^2}{2\pi/\Lambda}\right)\right|\right]\right\} \quad (5)$$

where J_p is the Bessel function of order p. Note that Eqs. (4) and (5) are derived from Eqs. (1)–(3) in a perturbation limit, namely whenever $|\beta_{2amp}/\beta_{2av}| \ll 1$ [7,17]. Therefore it is particularly interesting to study the domain of their validity in situations where the amplitude of the dispersion oscillations is equal or even much larger than the average dispersion. Note that indeed dispersion managed transmission systems almost always operate in the so-called strong management regime, namely the condition $|\beta_{2amp}/\beta_{2av}| \gg 1$ holds, which is precisely the opposite of the domain of validity of the perturbation theory that permits to derive Eqs. (4), (5).

3. Influence of the amplitude of the dispersion fluctuation

We start our study by investigating the influence of the amplitude of dispersion fluctuations β_{2amp} (or the corresponding D_{amp}) on the MI spectrum which is recorded after 12 spatial periods, i.e., a propagation distance of 12 km. Results are plotted in Fig. 1 for three levels of the amplitude of GVD oscillations, namely

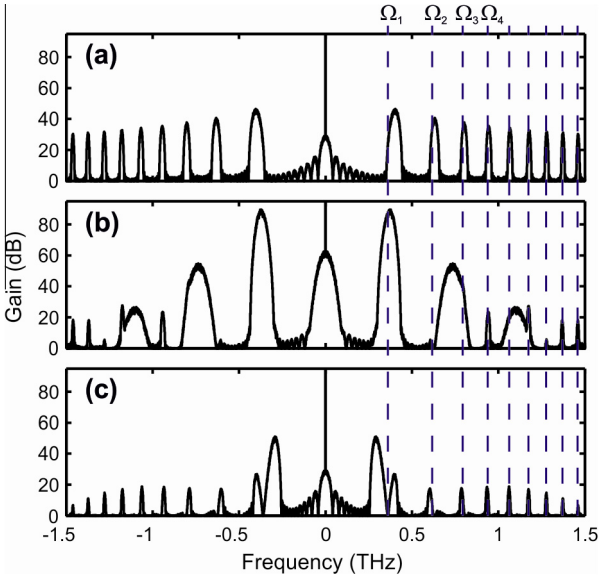

Fig. 1. Evolution of the output spectra recorded after 12 km of propagation for different values of the amplitude of the dispersion fluctuation: $D_{amp} = 0.5$, 1.7 and 3.7 ps/km/nm, subplots (a), (b) and (c) and respectively. The vertical dashed lines represent the predictions from Eq. (4).

$D_{amp} = 0.5$, 1.7 and 3.7 ps/km/nm, see subplots (a), (b) and (c), respectively. Our motivation in varying the amplitude of the dispersion oscillations rather than other parameters (such as the average dispersion or the longitudinal period, for example) is that a modification of the dispersion amplitude β_{2amp} should in principle have no influence, on the basis of Eq. (4), on the position of the MI sidebands.

Indeed, for a relatively low level of dispersion fluctuations, that is $D_{amp} = 0.5$ ps/km/nm (case (a) of Fig. 1), we observe the generation of unequally spaced and narrow spectral sidebands, whose position is in qualitative agreement with the analytical predictions of Eq. (4) (see dashed vertical lines). The possibility of observing QPM-induced MI in such a situation, where a large set of spectral lines is generated, was experimentally confirmed in the work of Droques et al. [5].

However, for an increasing level of dispersion amplitude oscillations (e.g., $D_{amp} = 1.7$ ps/km/nm, case (b) of Fig. 1), we observe two main features that lead to a very different structure of the output MI spectrum. We first notice from Fig. 1(b) that some of the spectral lines (for example, the lines corresponding to $p = 2$ or $p = 5$) have disappeared from the MI spectrum. Moreover, we may also point out in Fig. 1(b) the development of a new set of regularly spaced sidebands with a broader bandwidth. The first feature is explained by the evolution of the gain coefficient according to Eq. (5) which leads, for some values of the argument, to the annihilation of the sideband amplitude, as it was already confirmed experimentally in [11]. On the other hand, the second feature is linked to FWM between the pump wave and the first QPM sideband, and the subsequent cascading of the FWM process, as it was previously discussed and demonstrated experimentally in [9].

For an even higher amplitude of the dispersion oscillations, i.e. $D_{amp} = 3.7$ ps/km/nm (case (c) in Fig. 1), we observe instead of a single gain sideband, the unexpected emergence of a pair of sidebands around the angular frequency Ω_1. The emergence of the new pair of sidebands is not explained by nonlinear mixing between the various other sidebands, but it is an intrinsic property of the MI gain spectrum of Eqs. (1) and (3) in the strong dispersion management regime.

To verify this statement, we may write the perturbed CW solution of the NLSE (1, 3) as $\psi(z,t) = [\sqrt{P} + u(z,t)]\exp\{iPz\}$, where we

Download English Version:

https://daneshyari.com/en/article/462396

Download Persian Version:

https://daneshyari.com/article/462396

Daneshyari.com